On-chip Axicon for Light Sheet Microscopy

Alejandro Diaz Tormo and Nicolas Le Thomas

Photonics Research Group, Department of Information Technology, Ghent University - imec &
Center for Nano- and Biophotonics, Ghent University

Light sheet microscopy enables fast wide-field live cell imaging compared to confocal microscopy. To simplify the alignment procedure of this technique, we propose to generate the light sheet with an axicon lens integrated on a silicon nitride chip. We designed an axicon that generates light sheets with 2λ *resolution. Besides, in line with Huygens principle, we discuss the possibility to replace the axicon by an array of waveguides acting as point sources.*

1. Introduction

Axicon lenses are commonly used for optical trapping [1], laser microdrilling [2] and microscopy [3], among other applications. They exploit the non-diverging and self-healing nature of beams created by axicons [4].

In light sheet microscopy an axicon lens generates a plane illumination to reduce background noise while imaging a wide field of view. In combination with fluorescence dyes, it requires lower excitation intensities compared to other fluorescence imaging techniques for identical image acquisition times and spatial resolutions. It is therefore employed in long exposure studies where a high dose of light exposure could damage the sample.

In most studies, the axicon is assumed to be thin and the impact of secondary lobes is overlooked since they decay rapidly with the distance to the optical axis. The resulting beam is then defined as an approximation of a Bessel function of the first kind.

Our approach is based on the axicon on-chip illustrated in Figure 1. In contrast to conventional axicons, the planar axicon under consideration lacks revolution symmetry and, in turn, the output beam will not resemble a Bessel beam with decaying secondary lobes —it will instead form a light sheet.

The on-chip approach offers an intrinsically stable framework with the additional advantage that it is easy to place in an otherwise bulky system of lenses. We investigate the on-chip axicon on a silicon nitride platform since it is transparent for visible wavelengths, which makes it useful for biological applications. Water absorption in cells and tissues dictates the upper limit on the wavelength that can be used, ruling out the more common silicon platform with its corresponding longer wavelengths.

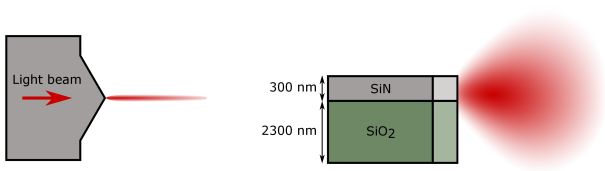

Figure 1: Top view (left side) and side view (right side) of the axicon on-chip showing the light sheet.

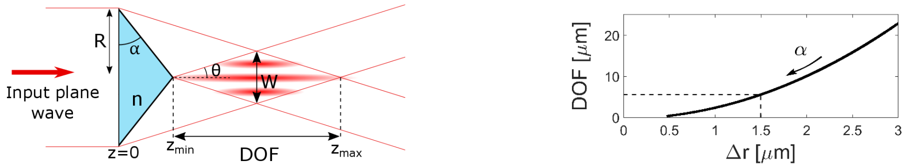

(a) (b)

Figure 2: (a) Axicon and light sheet parameters. Main and secondary lobes are also shown. (b) Depth of field against resolution of the light sheet generated with the proposed axicon for $\lambda = 0.78$ μm and n = 1.72. As indicated by the arrow, the Δr and DOF decrease when α is increased. Dashed lines indicate the values chosen for our design, $\Delta r = 1.5$ μm and a DOF = 5.57 μm.

In order to tailor the axicon properties, a variety of modifications has been proposed [5, 6]. Following on these ideas, we propose a novel structure integrated on chip based on an array of waveguides that would reproduce an axicon-like wavefront.

It is known that a limited width and typically the Gaussian profile of the input beam lead to a beam intensity that depends upon its distance to the axicon. This new approach could be used to address that issue.

In the following section we describe a mathematical model for the axicon lens. That model will be used in section 3 for the design of our axicon on-chip. And then, in section 4 we investigate the proposed structure based on an array of waveguides.

2. Axicon analysis

We first analysed the features of the axicon lens within the ray approximation, which holds as long as the input beam width and the axicon dimensions are many times larger than the wavelength. No restrictions on the size or shape of the axicon are applied as in the thin-axicon case.

The axicon parameters depicted in Figure 2.(a) are: internal angle α, refractive index n and radius R. We can assume that R is the input beam radius for all practical purposes. In contrast to Bessel beams, the 2D axicon entails secondary lobes that we have to consider in our model as they possess an amplitude similar to the main lobe.

From the axicon parameters we can derive, based on geometric considerations, the resulting beam properties of interest: depth of field DOF, maximum beam width W and maximum number of lobes #Lobes.

$$\mathrm{DOF} = z_{max} - z_{min} = \mathrm{R}(1/\tan\theta - \tan\alpha) \quad (1)$$

$$\mathrm{W} = \mathrm{DOF}\cdot\tan\theta = \mathrm{R}(1 - \tan\theta\tan\alpha) \quad (2)$$

$$\#\mathrm{Lobes} = \mathrm{W}/\Delta r \quad (3)$$

Where θ is the output beam divergence angle given by $\theta = \sin^{-1}(\mathrm{n}\sin\alpha) - \alpha$. z_{min} and z_{max} are the points indicated in Figure 2.(a), defined as $z_{min} = \mathrm{R}\cdot tan\alpha$ and $z_{max} = \mathrm{R}/tan\theta$, respectively. To define the resolution Δr we will adopt the Abbe criterion $\Delta r = \lambda/(2\sin\theta)$.

Equations (1) to (3) together with the Abbe criterion result in a trade-off between the DOF and Δr illustrated in Figure 2.(b). We can also see the impact of angle α. Small

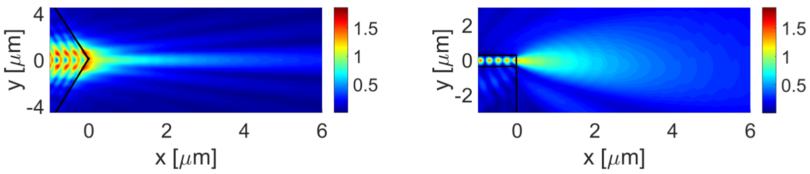

Figure 3: 3D FDTD simulation results for an axicon on-chip with R = 1.57 μm and $\alpha = 19.02^o$. The color scale indicates the electric field magnitud values for the fundamental TE mode of unitary amplitude. On the left the top view is shown and on the right the side view. Thick black lines indicate the structure boundaries.

α values mean that the input and output interfaces are almost parallel and therefore the input plane wave will not be focused. In the opposite case, for a large angle α between interfaces, the upper and lower halves of the beam will be refracted towards the optical axis. The interference of beams with abrupt angle of incidence yields better resolution at the expense of decreasing the DOF. The critical angle in Snell's law of refraction limits the maximum attainable α value ($\alpha_{crit} = \sin^{-1}(1/\mathrm{n})$) as well as the resolution.
In order to maintain the output beam free of secondary lobes it suffices to make sure that the beam width matches the resolution value. This statement is supported by Equation 3. The idea is to keep the beam radius R small enough to reject the secondary lobes, but as big as possible to get a long DOF.

3. Design

We designed an axicon on-chip especially for light sheet microscopy applications, which requires to work without secondary lobes that could hinder the advantages of a plane illumination. As previously mentioned, the wavelength and refractive index are constrained for biological applications. Namely, we will work at a wavelength of $\lambda = 780$ nm. We investigate the structure on a silicon nitride platform (300 nm silicon nitride layer on top of a 2.3 μm silicon oxide substrate). According to Finite-Difference Time-Domain (FDTD) simulations it features an effective refractive index of n $\simeq$ 1.72.
As indicated in Figure 2.(b), we chose to work with a resolution of 1.5 μm and a DOF of 5.57 μm. From these we can obtain the two remaining parameters to complete the design, R = 1.65 μm and $\alpha = 19.02^o$. Figure 3 shows a 3D simulation of the resulting light sheet. The resolution or width of the light sheet agrees with the design, however, as the profile along the x-axis is not constant, it would not make sense to compare the DOF obtained from the simulations with the expected designed value.

4. Engineered axicon

Using integrated photonics to create a light sheet offers the opportunity to scan it by on-chip dynamic phase control. One solution is to use an array of waveguides with adjustable amplitude and phase shifts to engineer the wavefront. Modulators on-chip could separately tune the amplitude and phase of each waveguide. The ability to change the wavefront in real time would make the structure versatile for multiple applications.
Huygens principle states that any wave can be decomposed in a set of spherical waves, each with a particular amplitude and phase. If we consider the waveguides as distinct

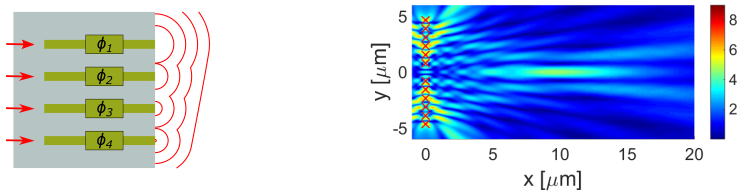

Figure 4: Left - Illustration of the Huygens principle where multiple waveguides generate a tilted plane wave. A phase delay ϕ_i is applied to each waveguide, where $\phi_i = i \cdot \phi_0$ and ϕ_0 is a constant phase. Right - FDTD simulation of two plane waves generated by point sources (red crosses) imitating the axicon behaviour.

point sources we could therefore generate any wavefront. Figure 4 illustrates how the Huygens principle works and shows a simulation based on the envisioned photonic structure. For simplicity reasons we used single point sources instead of waveguides. A fixed phase step between consecutive sources produces a beam that is seemingly generated by an axicon (top and lower sources are considered separately).

The non-constant intensity profile along the optical axis of beams generated by axicons is a documented issue. It could hinder the performance of the system and complicate the image retrieval of the sample. According to [5], the axial intensity profile can be tailored by means of a complex modulation of the field, using for instance a spatial light modulator. This new approach does exactly that and, therefore, it should be capable of achieving a constant axial intensity profile.

5. Conclusion

We have established a simple mathematical framework within the ray approximation containing all the relevant parameters of an axicon lens. It can be used to design on-chip axicons for light sheet microscopy among other applications. In future work we will validate the presented simulation results by fabricating and characterizing an axicon on-chip with the aforementioned parameters.

On the other hand, the proposed arrayed waveguide structure could further simplify the alignment process and offers a solution to scan the light sheet across the sample. Additionally, it could be used to correct the non-constant axial intensity profile characteristic of conventional axicons.

References

[1] V. Garcés-Chávez et al., "Simultaneous micromanipulation in multiple planes using a self-reconstructing light beam", *Nature*, vol. 419, pp. 145-147, 2002.

[2] Y. Matsuoka et al., "The characteristics of laser micro drilling using a Bessel beam", *Applied Physics A*, vol. 84, no. 4, pp. 423-430, 2006.

[3] W. Lemon et al., "Whole-central nervous system functional imaging in larval Drosophila", *Nature communications*, vol. 6, pp. 1-16, 2015.

[4] Z. Bouchal et al., "Self-reconstruction of a distorted nondiffracting beam", *Optics Communications*, vol. 151, pp. 207-211, 1998.

[5] T. Čižmár et al., "Axial intensity shaping of a Bessel beam", in *Proceedings of SPIE, Optical Trapping and Optical Micromanipulation VI*, 2009 vol. 7400

[6] O. Brzobohatý, et al., "High quality quasi-Bessel beam generated by round-tip axicon", *Optics Express*, vol. 16, no. 17, pp. 12688-12700.